An Artificial Viscosity Model and Boundary Condition Implementation of Finite Volume Methods for the Euler Equations

Wang Lei Zhuang Fenggan

Institute of Fluid Mechanics, BIAA, China

Abstract

The paper analyses the artificial viscosity model used in the explicit multistage finite volume methods for the solutions of the Euler equations, and suggests an alternative way to determine the coefficients contained in the model. The modified approach is applied to calculate transonic flows around airfoils, and the dependence of the numerical results on the magnitude of the artificial dissipations is examined. In addition, the effects of implementation of boundary conditions are discussed.

1. Introduction

The explicit multi-stage finite-volume methods developed by Jameson, Schmidt, and Turkel[1] are in wide use for numerical simulations of many complicated transonic flows. The 2D Euler equations in integral form are written as

$$\frac{\partial}{\partial t}\iint_V q\, dv + \int_{\partial\Omega} \vec{H}\cdot\hat{n}\, ds = 0 \qquad (1)$$

where $q = \begin{bmatrix} \rho \\ \rho u \\ \rho v \\ \rho E \end{bmatrix}$, $\vec{H} = F\,\hat{e}_x + G\,\hat{e}_y = \begin{bmatrix} \rho\vec{V} \\ \rho u\vec{V} + p\hat{e}_x \\ \rho v\vec{V} + p\hat{e}_y \\ (\rho E + p)\vec{V} \end{bmatrix}$

and $\vec{V} = u\,\hat{e}_x + v\,\hat{e}_y$

To discretize Eq.(1), central differences are applied to the spatial derivatives, and the resulted semi-discretized temporary differential equations are

$$\frac{\partial}{\partial t}(h\,q) + Qq - Dq = 0 \qquad (2)$$

where h stands for the area of an elementary quatrilateral cell in the flow field, Q stands for the central difference operator, and the artificial viscosity term Dq is explicitly added to maintain the numerical stability and eliminate nonphysical solutions. The additional dissipation, a blend of the second- and forth-order differences, is composed of two separate 1D operators, respectively, along subscripts i,j. For instance, in i's direction, it follows as

$$D_{ij}q = d_{i+\frac{1}{2}j} - d_{i-\frac{1}{2}j}$$

$$d_{i+\frac{1}{2}j} = (h_{i+\frac{1}{2}j} / \Delta t^{*}_{i+\frac{1}{2}j})\,[\epsilon^{(2)}_{i+\frac{1}{2}j}(q_{i+1j} - q_{ij}) - \epsilon^{(4)}_{i+\frac{1}{2}j}(q_{i+2j} - 3q_{i+1j} + 3q_{ij} - q_{i-1j})] \qquad (3)$$

and $\epsilon^{(2)}_{i+\frac{1}{2}j} = k^{(2)} \max(\nu_{i+1j}, \nu_{ij})$

$$\epsilon^{(4)}_{i+\frac{1}{2}j} = \max(0,\ k^{(4)} - \epsilon^{(2)}_{i+\frac{1}{2}j})$$

where $h_{i+\frac{1}{2}j}$ is the area averaging of two neighbouring cells for the cell edge $S_{i+\frac{1}{2}j}$, and the introduction of the factor $h_{i+\frac{1}{2}j}/\Delta t^{*}_{i+\frac{1}{2}j}$ preceding to the square bracket is, according to Ref. [1], reasoned as to make the artificial dissipation terms dimensionally consistent with others. The time interval $\Delta t^{*}_{i+\frac{1}{2}j}$ is determined so that it brings about a local Courant number of unity. But a question arises as that for the above established scheme applied to the multi-dimensional Euler equations, no formula is rigoriously given to define Courant number, via which to determine Δt, and it seems worse that for some other references using Jameson et al. schemes, two time steps, one occurring in the artificial viscosity term and another used for the time integration, are misunderstood as the same, and this would lead to an erroneous impression that owing to the dependence of the converged steady-state solutions on both the spatial central differences and the artificial viscosity terms, and the inclusion of the time marching step Δt in the later, the variation of the artificial viscosity due to the change of Δt will result inevitably the change of the converged steady-state solutions. In order to avoid such misunderstanding, in the present paper, we built up the numerical approximate fluxes, instead of two parts- the central differences and the artificial dissipations in the Jameson et al. schemes - to discretize the spatial derivatives in Eq.(1), and the factor preseding to the equivalent dissipation difference terms in so-defined numerical fluxes is evaluated by analogy to the physical based upwind schemes. In addition, the effects of the different implementation of the wall boundary conditions on the numerical results are discussed.

2. Numerical Approximate Fluxes

From the point view of physics, upwind schemes based upon the assumption of the characteristics theory and wave propagation maintain the flow information transfer in reality. Pullian[2] analysed the common points of upwind schemes and central difference one, and concluded that for the discretization of the spatial derivatives of the Euler equations, the application of the second-order upwind schemes has the same function as using central differences with the addition of a forth-order dissipation term, and the first-order upwind schemes equivalent to the central differences plus a second-order dissipation. The coefficients of the appended viscosity terms should be some sort of flux Jacobian scaling. The comprehensive numerical experiments[1-4] using central difference schemes with addition of the artificial viscocity term , and some recent work applying flux limiters to upwind schemes[5] and TVD concepts[6] suggest that the optimised approaches to establish the efficient shock-capturing schemes are to use a locally first order schemes at shock waves and the second-order elsewhere. For the algorithm using central differences to discretize the spatial derivatives, this can be accomplished by a switch operator to control the action of the second- and forth-order dissipation as applied to finite volume methods, such appended artificial dissipation can be introduced by a corrected numerical fluxes, instead of the standard second-order difference ones, for the Euler fluxes in Eq.(1).Consider flux through $\Delta S_{i+\frac{1}{2},j}$, an edge of cell i,j, F. It can be numerically calculated as

$$F_{i+\frac{1}{2},j} = \frac{1}{2}(F_{i+1,j} + F_{i,j}) +$$

$$\sigma_{i+\frac{1}{2},j}[\epsilon^{(2)}(q_{i+1,j} - q_{i,j}) - \epsilon^{(4)}(q_{i+2,j} - 3q_{i+1,j} + 3q_{i,j} - q_{i-1,j})] \quad (3)$$

where $\Psi(F_{i+1,j}, F_{i,j})$ is some symmetric averaging of $F_{i,j}$ and $F_{i+1,j}$, and for the purpose of numerical efficiency, a simplist averaging is used as

$$\Psi(F_{i+1,j}, F_{i,j}) = 1/2\ (F_{i,j} + F_{i+1,j})$$

the second term is the appended dissipation, the coefficients of which, as stated before, is taken as the spectral radius of local flux Jacobian $\tilde{A}$, i.e.,

$$\sigma = \rho(\tilde{A}) = |u_n| + a \quad (4)$$

and

$$\tilde{A} = A\, e_\xi^x + B\, e_\xi^y ,$$

$$u_n = u\, e_\xi^x + v\, e_\xi^y$$

where $\vec{n} = (e_\xi^x, e_\xi^y)$ is the unit normal to $\Delta S_{i+\frac{1}{2},j}$, a is speed of sound and A,B Jacobians of the flux functions F and G. It is worthwhile to note that the determination of σ here differs from the formula

$$\sigma = \rho(\tilde{A}) + \rho(\tilde{B})$$

as suggested in Ref.[2]. In the arbitrary non-orthogonal curvilinear coordinates, it seems reasonable to use formula (4). The testing functions of ν_{ij} in the artificial dissipations make possible that the resulted algorithm is the first-order at shock waves and the second-order elsewhere, and the introduction of the scaling of local pressure gradient further enhances the numerical stability.

3. Boundary Condition Implementation

For inviscid flows around airfoils, slipping condition is imposed on wall, i.e.,

$$(\vec{V}.\vec{n}) = 0 \quad (5)$$

where $\vec{n} = (n^x, n^y)$ is the outward normal to the wall. Applied to the finite volume methods, it makes flux function become

$$H \cdot n = \begin{pmatrix} 0 \\ p_w n^x \\ p_w n^y \\ 0 \end{pmatrix}$$

where p_w is the wall pressure, which can be calculated from the formula

$$\frac{\partial p}{\partial n} = K \rho u_\tau^2 \quad (6)$$

where K stands for the wall curvature, and u_τ approximated as the velocity component in the neighbouring cell along the wall tangent. For an airfoil profile defined by a closed analytical function, it is easy to calculate the curvature value of the wall. But for the airfoil profile stipulated by a set of discrete values, such as RAE2822, difficulties arise to evaluated accurately curvature values by some form of polynomial functions because of the existence of geometrical singularities of the airfoil near the leading edge. An alternative to determine the wall pressure is to apply the normal momentum equation,which takes the form,in curvilinear coordinates (ξ, η), as follows

$$\rho U(u\frac{\partial n^x}{\partial \xi} + v\frac{\partial n^y}{\partial \xi}) = \frac{1}{J}[(n^x \xi_x + n^y \xi_y)\frac{\partial p}{\partial \xi} + (n^x \eta_x + n^y \eta_y)\frac{\partial p}{\partial \eta}] \quad (7)$$

When the curvilinear coordinates are nearly orthogonal in the neighbourhood of the wall, which means that

$$n^x \xi_x + n^y \xi_y = 0$$

Eq.(7) can be simplified as

$$\rho U(u\frac{\partial n^x}{\partial \xi} + v\frac{\partial n^y}{\partial \eta}) = \frac{r}{J}\frac{\partial p}{\partial \eta} \quad (8)$$

and $U = u\,\xi_x + v\,\xi_y$,

$r = (\eta_x^2 + \eta_y^2)^{1/2}$

Where $\vec{n}=(\eta_x, \eta_y)/r$ is the unit normal of the wall, and J the Jacobian value of the coordinate transformation. Using the first-order difference quotient to approximate $\frac{\partial P}{\partial x}$, and determining other values in the same way as before, the pressure on the wall can be easily evaluated.

4. Numerical Results and Discussion

Three pairs of different values $k^{(2)}$, $k^{(4)}$ are separately used to calculate the transonic flow around NACA0012 airfoil at M =0.8 and ALFA=1.25deg., where ALFA stands for the angle of attack. In Tab.1, aerodynamic coefficients and the maximum and minimum of the pressure coefficients are given, and Fig. 1 displays the pressure coefficient along the chordwise direction. It is clear that the position of shock waves obtained using different values of $k^{(2)}$, $k^{(4)}$ are nearly the same, where x =0.624 for the shock wave on the upper surface. When the large value of $k^{(2)}$, $k^{(4)}$ are taken, the profile of shock waves are slightly smoothed, and for the present case it spans six grids. Post-expansion of inviscid flow just downstream of the shock wave is damped out. When taking the smaller values of $k^{(2)}$, $k^{(4)}$, evidently there exist preshock and postshock oscilations. When the adequate values are taken, for instance the second pair values, such spurious oscilations are completely eliminated, and the profile of the shock waves on the upper surface, spanning only four grids, is satisfactory. Just downstream of the shock wave occurs the post expansion, which shows clearly the behaviour of inviscid flows through shock waves stemming from a curved wall.

NACA0012 airfoil M=.8, A=1.25					
k	k	Cpmin	Cpmax	CL	CD
.25	.005	-1.1357	1.1319	.3479	.0215
1.0	.032	-1.1146	1.174	.3525	.0226
2.0	.064	-1.1213	1.2091	.3571	.0238

Tab.1 Computed results for NACA0012 airfoil witn M=.8, A=1.25deg.

B. C.	Cpmin	Cpmax	CL	CD
Eq.(5)	-1.0101	1.1823	.3548	.0556
Eq.(8)	-1.0111	1.1792	.3438	.0542

Tab.2 Computed results for NACA0012 with M=.85, A=1.0 deg.

M	A	Cpmin	Cpmax	CL	CD
.725	2.55	-1.4453	1.0859	.6341	.0384
.75	3.0	-1.4826	1.084	1.0316	.0422

Tab.3 Computed results for RAE2822

Two different ways to implement the boundary condition on the wall are used to calculate the transonic flow around NACA0012 airfoil at M =.85 and ALFA= 1.0. Tab. 2 gives aerodynamic coefficients and the maximum and minimum of the pressure coefficient and, Fig.2 displays the pressure coefficient along the chordwise direction. Two results are nearly equivalent. Some other examples using Eq.(8) to evaluate the wall pressure are the transonic flows around RAE2822 airfoil. Their results are given in Tab. 3 and Fig 3. All of these examples show that the approaches used in the present paper to implement the wall boundary conditions are suitable.

5. References:

(1) Jameson,A., Schmidt,W. and Turkel,E. , AIAA Paper 81-1259,(1981)

(2) Pulliam, T.H.,AIAA Paper 85-0438,(1985).

(3) Steger,J.L., AIAA paper 77-665,(1977).

(4) Osher,S.,and Chakravarthy,S. J. Comp. Phys.,50, (1983),447-481.

(5) Harten,A, J. Comp. Phys.,49,(1983),375-393.

(6) Oswatitsh, K, Transonic Flow, Theoretical and Applied Mechanics,Koiler, W.T. ed., North-Holland Publishing Company(1976).

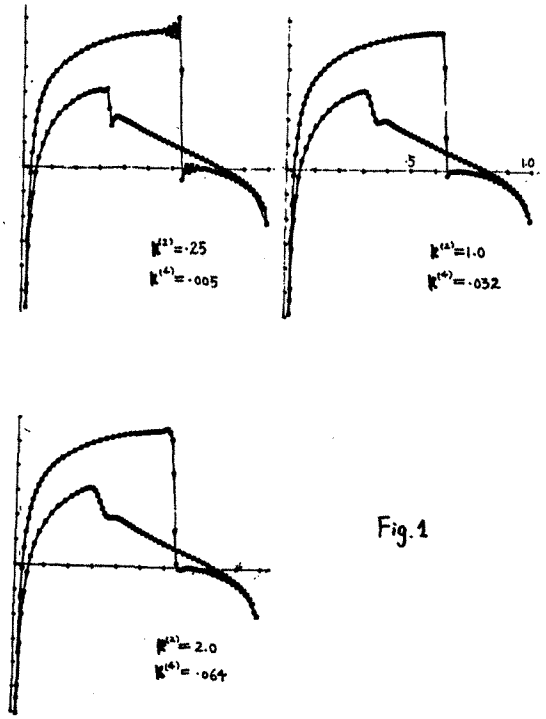

Fig.1

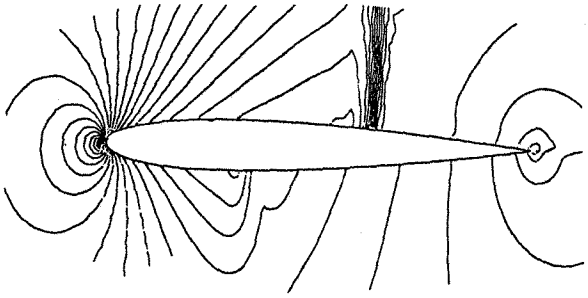

(a) Mach number contours

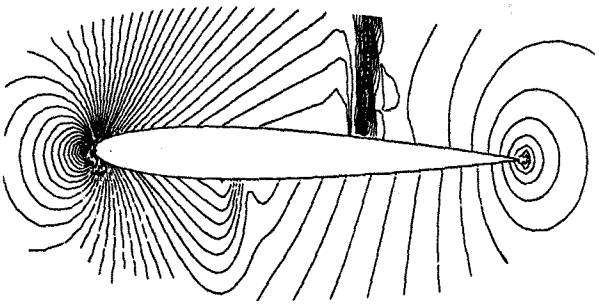

(b) Iso-bar contours

Fig. 1 (Continue)

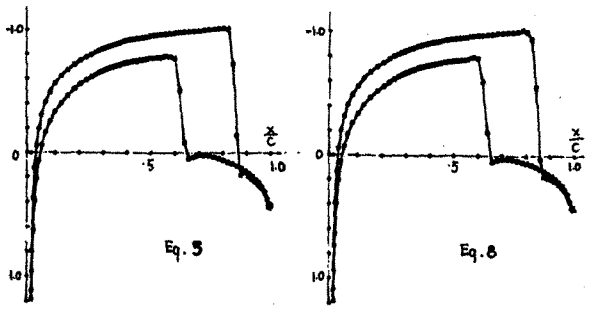

Fig. 2

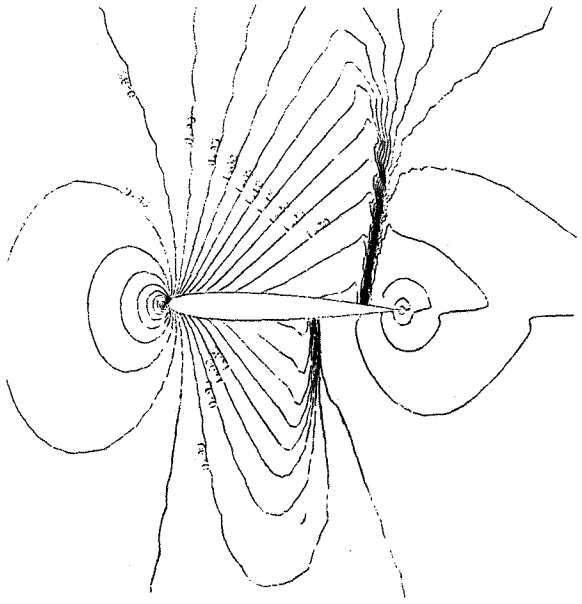

(a) Mach number contours

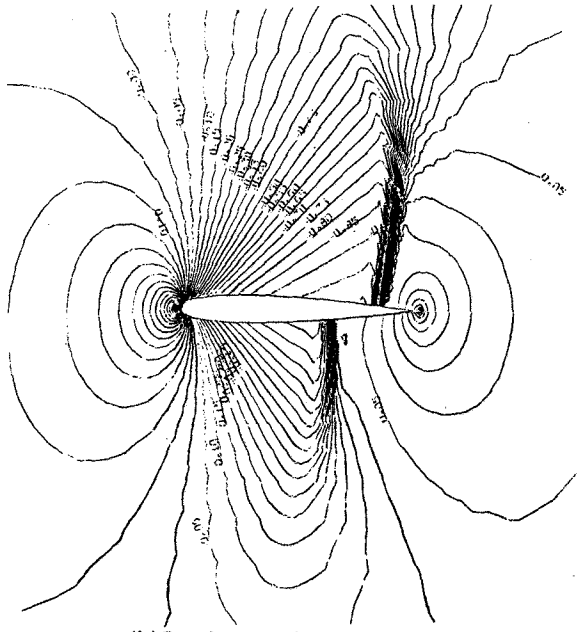

(b) Iso-bar contours

Fig. 2 (Continue)

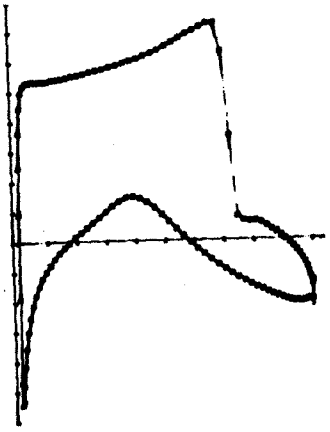

MACH number= 0.725

ALF= 2.55 deg.

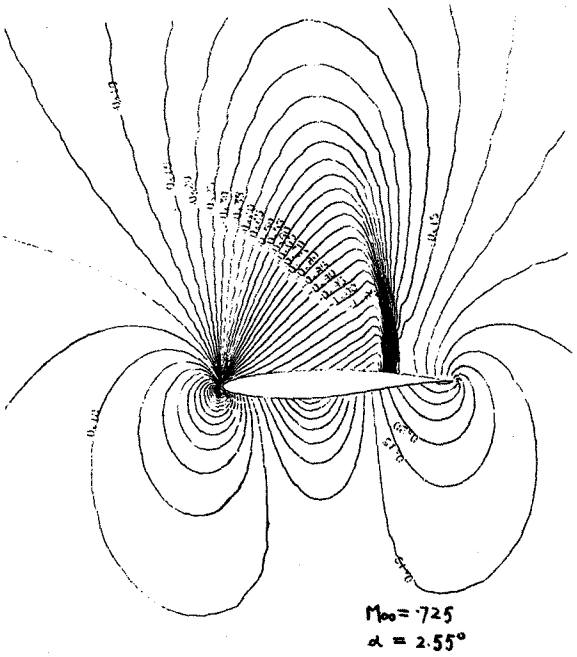

(b) Iso-bar contours

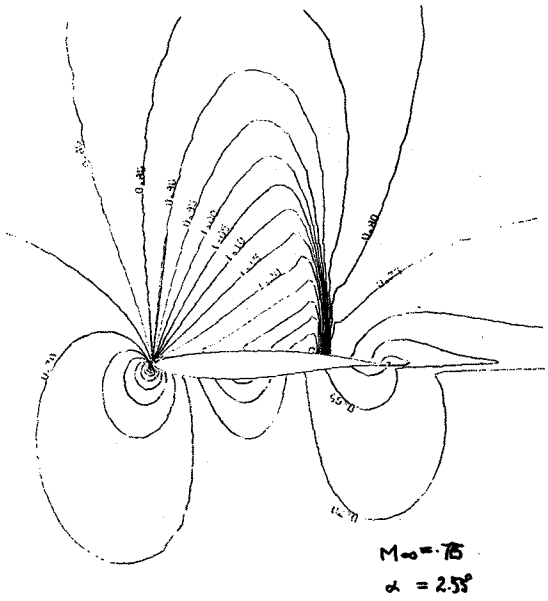

(a) Mach number contours

Fig. 3

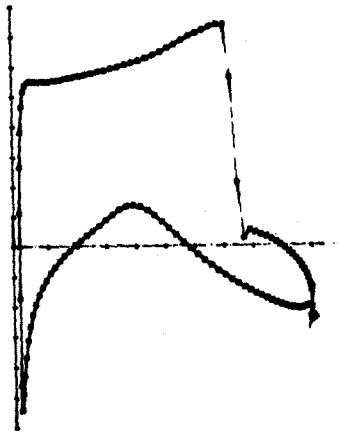

MACH number= 0.75

ALF= 3.0 . deg.

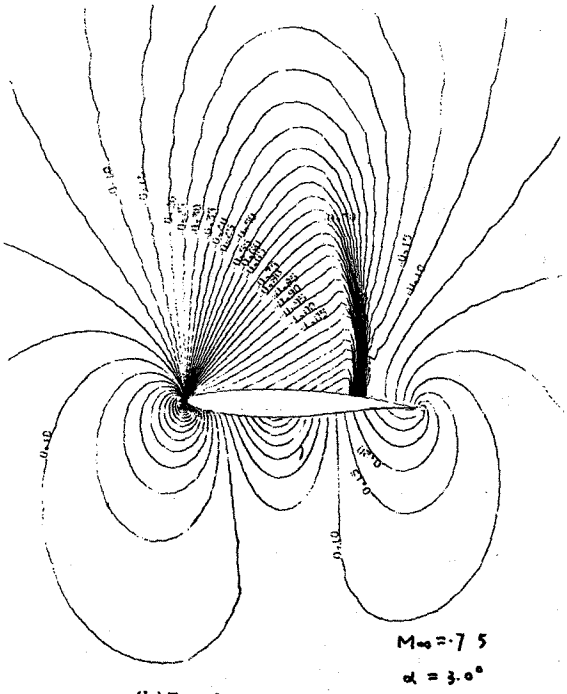

(b) Iso-bar contours

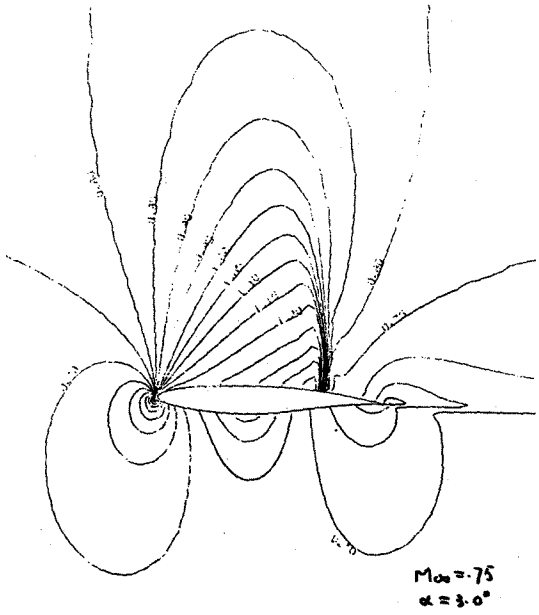

(a) Mach number contours

Fig. 3 (Continue)